Coupling of Hydrodynamics and Chemical Reaction in Gas-Lift Reactors

M. A. Márquez, A. E. Sáez, R. G. Carbonell, and G. W. Roberts
Dept. of Chemical Engineering, North Carolina State University, Raleigh, NC 27695

A model was developed to study the strong coupling between hydrodynamics and chemical reaction that occurs in external-loop gas-lift reactors. The model predicts the liquid circulation rate, as well as the axial profiles of gas holdup, pressure, gas and liquid velocity, and reactant conversion in the riser. The study on the first-order, irreversible, isothermal reaction in the gas phase $nA \xrightarrow{k} B$ *with a change in the number of moles on reaction shows that for* $n > 1$*, the gas holdup decreases along the riser, the liquid circulation rate is lower than that in the absence of reaction, and liquid circulation decreases as n and k increase. The bubble radius at the sparger and the inlet gas composition can have important effects on reactor performance. Scale-up strategies that involve increasing the reactor length result in higher reactant conversion, but a lower ratio of liquid circulation rate to gas feed rate.*

Introduction

The distinguishing feature of a gas-lift reactor (GLR) is the liquid circulation that is created by the gas feed. Figure 1 is a diagram of the external-loop GLR used by Young et al. (1991) and Amend (1992). The gas that enters at the sparger and leaves the top of the gas/liquid separator induces a circulatory flow of liquid up the riser, through the separator, and down the downcomer. The fact that liquid circulation is achieved with no moving parts such as a pump makes GLRs particularly useful in certain applications. For example, the high-velocity environment of a pump could damage shear-sensitive biomass or polymers, and could cause attrition of solid catalysts. Moreover, in a corrosive or erosive system, a pump could be a major source of reliability and/or maintenance problems. The liquid circulation in a GLR also gives rise to some related advantages such as simple mechanical design, low power consumption, and nearly isothermal operation.

Gas-lift reactors have been used primarily in biological applications such as fermentation, where gas/liquid mass transfer and reaction are relatively slow. Consequently, almost all fundamental hydrodynamic studies of GLRs have involved nonreacting systems such as the air-water system, and virtually all hydrodynamic models ignore chemical reaction and gas/liquid mass transfer. However, the potential utility of gas-lift reactors is not limited to slow oxidation reactions. Amend (1992) and Fleischer et al. (1996) used GLRs to carry out the reaction between aqueous solutions of a strong base (such as NaOH and KOH) and gaseous CO_2. In both studies, there was a substantial reduction in gas holdup along the riser as CO_2 was consumed. This gas consumption affected the hydrodynamics of the reactor significantly, especially the rate of liquid circulation. A similar situation might exist in any GLR that was used for a reaction involving CO and/or H_2, for example, Fischer-Tropsch synthesis, methanol and methyl acetate carbonylation, and benzene hydrogenation.

The objective of the present work is to explore the coupling of hydrodynamics and chemical reaction in an external-loop GLR, that is, to understand how the hydrodynamic behavior of the GLR is altered by the occurrence and the characteristics of the reaction, and to understand how the behavior of the reaction is affected by the hydrodynamic variables. At first glance, it does not appear possible to approach these objectives with any degree of generality. Each reaction that might be run in a GLR has distinctly different characteristics. For example, gas may be produced as the reaction proceeds, as in the case of anaerobic digestion of biomass, or gas may be consumed, as in the previously-cited reactive adsorp-

Correspondence concerning this article should be addressed to G. W. Roberts.
Current address of M. A. Márquez: INTEVEP S.A., Apdo. 76343, Caracas 1070A, Venezuela.
Current address of A. E. Sáez: Dept. of Chemical and Environmental Engineering, University of Arizona, Tucson, AZ 85721.

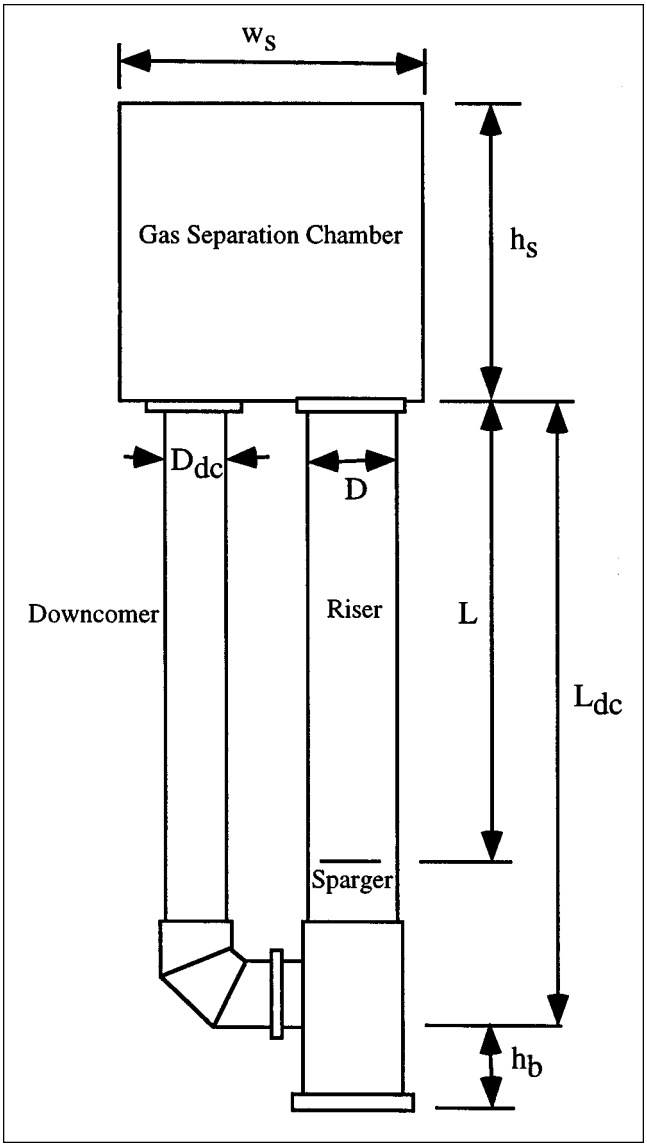

Figure 1. External loop GLR used by Young et al. (1991) and Amend (1992).

Dimensions in cm: $w_s = 70.5$; $h_s = 86.4$; $D_{dc} = 14.0$; $D = 19.0$; $L = 165$; $L_{dc} = 199$; $h_b = 10.5$. Width of gas/liquid separator chamber = 27.9.

tion of CO_2. The kinetics of each reaction will be different, as will the stoichiometry such as the number of moles of gas produced or consumed per mole of reactant consumed. If reactions occur in the liquid phase, mass transfer across the gas/liquid interface will have to be considered. The Fischer-Tropsch reaction involves a particularly complex set of reactions, mass-transport processes, and phase equilibria. The reactants CO and H_2 are transported from the gas into the liquid, where they react on the surface of a suspended solid catalyst. The products, primarily hydrocarbons with carbon numbers from 1 to about 100 and either CO_2 or H_2O, depending on the catalyst, are transported from the liquid into the gas phase. Multiple phase equilibria must be considered in order to determine how reactants and products partition between the phases.

For many real systems, the number of expressions that are required to describe stoichiometry, reaction kinetics, mass transport, and phase equilibrium can be large, even for an isothermal system. Moreover, the number and variety of parameters that are required to model such systems can camouflage the fundamental physical phenomena that control system behavior. Some of the complexities of rigorously modeling a specific reaction are illustrated by the works of Fleischer et al. (1996) who developed an unsteady-state, 1-dimensional (1-D), nonisothermal, 2-phase model that is specific to the absorption of CO_2 into NaOH in either a bubble column or an external-loop GLR, and of Márquez (1999), who developed a pseudo-steady-state model for the reactive absorption of CO_2 into KOH.

The most significant effects of a chemical reaction on the hydrodynamics of a GLR, and *vice versa*, occur when the gas superficial velocity changes with axial position in the riser, as a result of net molar gas consumption or production as the reaction proceeds. Changes in the gas superficial velocity lead to changes in the gas holdup, the actual gas velocity, and the bubble size profile. These changes have a direct impact on the gas-phase continuity equation, the gas-phase momentum balance, and the liquid-phase momentum balance in the riser. On the other hand, the consumption or production of gas has a relatively small impact on the liquid-phase mass balance and liquid properties, since the mass-flow rate of gas in the riser is usually a small fraction of the mass-flow rate of liquid, at typical GLR operating conditions. Therefore, a great deal can be learned about the fundamentals of reaction/hydrodynamic coupling in a GLR by studying a model reaction that creates substantial changes in the gas superficial velocity, but does not involve the liquid phase. The irreversible, first-order, gas-phase reaction with mole change $nA \xrightarrow{k} B$ has exactly these characteristics. The stoichiometric coefficient n determines the maximum moles of gas that can be consumed or created. The reaction rate constant k determines the rate at which the asymptotic limit of gas consumption/production is approached. This simple model provides very useful insight into how the coupling between hydrodynamic and reaction parameters affects system performance, even though the model does not capture the complex mass-transfer and phase-equilibria effects that can occur in some systems.

Model Formulation

In a previous work (Sáez et al., 1998), a mathematical model was developed to describe the hydrodynamics of external-loop GLRs in the absence of chemical reaction. This model was a modification of an earlier one by Young et al. (1991). The Sáez et al. model is based on spatially-averaged, 1-D equations of continuity and momentum in the riser, and on macroscopic mechanical energy balances for the gas-liquid separator and external downcomer. The model predicts the rate of liquid circulation, and the axial profiles of gas holdup, pressure, and gas and liquid velocity for the bubbly-flow regime in the riser. The inputs required are the physical properties of the gas and liquid phases, the reactor dimensions, the inlet gas superficial velocity, and, for some cases, the bubble radius at the sparger. The predictions match the data and predictions of other authors (Young et al., 1991;

Merchuk and Stein, 1981; Chisti et al., 1988; Ghirardini et al., 1992).

The model of Sáez et al. (1998) has been extended to include the irreversible, first-order reaction with mole change $nA \xrightarrow{k} B$, which is assumed to take place isothermally in the gas phase. Both A and B are assumed to be insoluble in the liquid phase, so that there is no gas-liquid mass transfer and no change in the composition of the liquid phase. This eliminates the need to include liquid feed and removal streams which will, in general, influence the reactor hydrodynamics by adding a component to the liquid flow rate that is not connected directly to the liquid circulation induced by the gas flow. The GLR is assumed to operate at steady state. Only gas consumption ($n > 1$) is considered in this article.

The assumptions and equations that constitute the present model are described below. Those equations that are common with the earlier, no-reaction, model are summarized briefly, but are not derived again. Their complete development can be found in Sáez et al. (1998).

Riser

Continuity equations

Starting from the time-averaged point equation of continuity for each phase, an averaging process over a representative volume of gas-liquid suspension is carried out. The volume-averaged equations are then averaged over the cross-section of the riser. By assuming steady state, uniform gas and liquid density, and negligible gas-liquid mass transfer, the following equations are obtained

$$\text{Liquid} \qquad \rho_l(1-\bar{\epsilon})\langle \bar{v}_l \rangle = L_f \tag{1}$$

$$\text{Gas} \qquad \rho_g \bar{\epsilon} \langle \bar{v}_g \rangle = G \tag{2}$$

where ρ_l and ρ_g are the liquid and gas densities, respectively, and L_f and G are the liquid and gas mass fluxes in the riser, respectively. These fluxes are independent of axial position, and G is related to the inlet gas superficial velocity by $G = U_g^0 \rho_g^0$, where U_g^0 and ρ_g^0 are the inlet gas superficial velocity and gas density at the sparger, both evaluated at 298 K and 1 atm pressure.

In Eqs. 1 and 2, the angular brackets represent intrinsic phase averages of the z-component of the phase velocities

$$\langle v_i \rangle = \frac{1}{V_i} \int_{V_i} v_i \, dV, \qquad i = g, l \tag{3}$$

where V_i is the portion of the averaging volume occupied by phase i (m^3), v_i is the point velocity of phase i (m/s), and g and l denote the gas and liquid phases, respectively. The bars in the previous equation refer to cross-sectional averages such as

$$\langle \bar{v}_i \rangle = \frac{1}{A} \int_A \langle v_i \rangle \, dA \tag{4}$$

where A is the cross-sectional area of the riser (m^2).

The gas holdup is defined over a representative volume of gas-liquid suspension as

$$\epsilon = \frac{V_g}{V_g + V_l} \tag{5}$$

In the development of Eqs. 1 and 2, the terms that might give rise to dispersive contributions due to variations in the phase velocities throughout the cross-section have been neglected. These effects might be important in churn-turbulent flows, where the liquid phase exhibits a strong recirculation within the riser. Therefore, this analysis is restricted to bubbly flows, for which dispersive contributions are small with respect to the mean flow.

Momentum equations

The development of the momentum equations also starts from the time-averaged point equation of motion for each phase. An averaging process is carried out over a representative volume of gas-liquid suspension, and the volume-averaged equations are averaged over the cross-section of the riser. Assuming steady state, bubbly flow, uniform liquid density, no pressure jump between phases, negligible gravitational contributions in the gas phase, and negligible gas-liquid mass transfer leads to

$$\text{Liquid} \qquad -\frac{d\langle \bar{P} \rangle}{dz} - (1-\bar{\epsilon})\rho_l g - \frac{f_r \rho_l}{2D} \langle \bar{v}_l \rangle^2 = 0 \tag{6}$$

$$\text{Gas} \qquad \bar{\epsilon} \rho_l g = \bar{a}_{lg} \bar{F}_d$$

or alternatively

$$\bar{\epsilon} \rho_l g = \frac{\bar{a}_{lg} \hat{C}_d \rho_l}{8} \left(\langle \bar{v}_g \rangle - \langle \bar{v}_l \rangle \right) | \langle \bar{v}_g \rangle - \langle \bar{v}_l \rangle | \tag{7}$$

where P is the pressure (N/m^2), z is the axial distance (m) measured from the sparger, f_r is the two-phase riser friction factor, D is the riser diameter (m), $\bar{a}_{lg}$ is the gas-liquid interfacial area per unit volume of gas-liquid suspension (m^2/m^3), $\bar{F}_d$ is the gas-liquid drag force per unit interfacial area (N/m^2), C_d is the drag coefficient, and g is the acceleration due to gravity (m/s^2).

Empirical correlations are used to represent frictional and drag effects. The sensitivity of the model to the choice of the drag coefficient correlation has been analyzed by Sáez et al. (1998). When the drag coefficient is an explicit function of the Reynolds number, the bubble size at the sparger (r_{b0}) (m) must be known, and the model is sensitive to this value. Presumably, r_{b0} will depend on the geometry of the distributor, the physical properties of the phases, and the gas and liquid velocities. Once r_{b0} is known, the value of r_b at any position can be calculated by assuming no bubble break up or coalescence, which is reasonably valid for bubbly flow. For monodisperse bubbles

$$r_b = \left[\frac{\bar{\epsilon} \langle \bar{v}_g \rangle}{\left(\bar{\epsilon} \langle \bar{v}_g \rangle \right)_{z=0}} \right]^{1/3} r_{b0} \tag{8}$$

In the present work, the correlation

$$\hat{C}_d = \frac{24}{Re}\left(1 + 0.10\,Re^{0.75}\right)$$

was used for the drag coefficient (Ishii and Zuber, 1979). This correlation is valid for $Re < 2\times 10^5$.

Gas-Liquid Separator

Macroscopic mass balance

The volumetric liquid flow leaving the riser is equal to that entering the downcomer

$$\left[(1-\bar{\epsilon})\langle \bar{v}_l \rangle\right]_{z=L} A = \bar{v}_{dc} A_{dc} \tag{9}$$

where $\bar{v}_{dc}$ is the cross-sectional-area average of the liquid velocity in the downcomer, L is the length of the riser (m), and A_{dc} is the cross-sectional area of the downcomer (m^2). For simplicity, it is assumed that there is no gas in the downcomer, that is, that gas is disengaged completely in the gas/liquid separator.

Macroscopic mechanical energy balance

Following the arguments of Young et al. (1991), a macroscopic mechanical energy balance on the separator indicates that the pressure at the top of the riser ($\langle \bar{P} \rangle_{z=L}$) and the pressure at the top of the downcomer ($\langle \bar{P}_{dc} \rangle_{z=L}$) are approximately equal. Furthermore, it will be assumed that

$$\langle \bar{P} \rangle_{z=L} = P_{\text{atm}} + \rho_l g h_t \tag{10}$$

where h_t is the height of liquid in the gas/liquid separator (m).

Downcomer

Macroscopic mechanical energy balance

The downcomer consists of a pipe with single-phase flow of liquid, assuming that gas is completely disengaged in the gas/liquid separator. A macroscopic mechanical energy balance is performed on a control volume that extends from the top of the downcomer to the sparger in the riser. Detailed derivations presented elsewhere (Young et al., 1991; Sáez et al., 1998) lead to

$$\underset{\text{(downcomer to riser)}}{\overset{\text{kinetic energy change}}{\downarrow}} \frac{\bar{v}_{dc}^2}{2g}\left\{\left[\left(\frac{D_{dc}}{D}\right)^4 - 1\right] + \underset{\text{friction}}{\overset{\text{wall}}{\downarrow}} f_{dc}\frac{L_{dc}}{D_{dc}} + \underset{\text{losses}}{\overset{\text{accessories}}{\downarrow}} \sum_i K_i\right\} + \underset{\text{contribution}}{\overset{\text{pressure}}{\downarrow}} \frac{\langle \bar{P} \rangle_{z=0} - \langle \bar{P}_{dc} \rangle_{z=L}}{\rho_l g} - \underset{\text{contribution}}{\overset{\text{gravitational}}{\downarrow}} L = 0 \tag{11}$$

where f_{dc} represents the friction factor in the downcomer, D_{dc} is the downcomer diameter (m), and $\langle \bar{P}_{dc} \rangle_{z=L}$ is the pressure at the top of the downcomer. The term $\sum_i K_i$ represents the summation of all mechanical energy losses due to accessories (such as elbows, ''tees,'' expansions, and contractions). The same values for this term and for f_{dc} that were used by Young et al. (1991) and Sáez et al. (1998) were used in this work.

Relationship between Gas Holdup and Liquid Circulation

When $n \neq 1$, the chemical reaction causes changes in the gas holdup along the riser. The average or global gas holdup in the riser ϵ_g is defined as

$$\epsilon_g = \frac{1}{L}\int_0^L \bar{\epsilon}\, dz \tag{12}$$

There is a strong relationship between this global gas holdup and the liquid circulation rate. To understand this relationship, an approximate analysis of the liquid momentum equation is performed. If wall friction in the riser is small relative to the hydrostatic pressure change, Eq. 6 can be integrated from $z = 0$ to $z = L$ to obtain

$$\langle \bar{P} \rangle_{z=L} - \langle \bar{P} \rangle_{z=0} \approx -\int_0^L (1-\bar{\epsilon})\,\rho_l g\, dz = -(1-\epsilon_g)\,\rho_l g L \tag{13}$$

Equation 13 is not universally valid, since wall friction can be a significant fraction of the hydrostatic pressure change when $\bar{\epsilon}$ and $\langle \bar{v}_l \rangle$ are large (Young et al., 1991). The downcomer mechanical energy balance Eq. 11 can be written as

$$C(\bar{v}_{dc}, \text{Ge})\frac{\bar{v}_{dc}^2}{2g} + \frac{\langle \bar{P} \rangle_{z=0} - \langle \bar{P} \rangle_{z=L}}{\rho_l g} - L = 0 \tag{14}$$

where $C(\bar{v}_{dc}, \text{Ge})$ is the sum of the terms in the {} brackets of Eq. 11. The parameter $C(\bar{v}_{dc}, \text{Ge})$ is a function of $\bar{v}_{dc}$ because the friction factor f_{dc} depends on the velocity in the downcomer, and is a function of the geometry of the system, as indicated by the symbol Ge. Equation 14 contains the approximation that $\langle \bar{P}_{dc} \rangle_{z=l} = \langle \bar{P} \rangle_{z=L}$, as discussed above in connection with the gas/liquid separator.

Combining Eqs. 13 and 14 gives

$$\bar{v}_{dc} = \left[\frac{2g\epsilon_g L}{C(\bar{v}_{dc}, \text{Ge})}\right]^{1/2} \tag{15}$$

There are several limiting cases of Eq. 15. First, consider a given reactor, that is, a fixed geometry. In turbulent flow, f_{dc} is a weak function of $\bar{v}_{dc}$. For that situation, Eq. 15 yields

$$\bar{v}_{dc} \propto \epsilon_g^{1/2} \tag{16a}$$

Equation 16a shows that if the global gas holdup in the riser

decreases due to chemical reaction, the liquid circulation rate will decrease almost in proportion to $\epsilon_g^{1/2}$.

When the geometry of the GLR changes, there are two limiting forms of Eq. 15 that help to illuminate the effect of riser length L on the liquid circulation rate. First, if the frictional losses in the downcomer are small compared to the accessories losses plus the kinetic energy change, then $C(\bar{v}_{dc},\mathrm{Ge})$ will be a weak function of L_{dc}. For constant riser and downcomer diameters

$$\bar{v}_{dc} \propto (\epsilon_g L)^{1/2} \tag{16b}$$

This equation will apply to relatively short GLRs, as long as changes in L_{dc} do not cause the term $f_{dc}L_{dc}/D_{dc}$ to become significant relative to the sum of the other terms in $C(\bar{v}_{dc},\mathrm{Ge})$. Equation 16b shows that the liquid circulation rate will increase with L unless there is a compensating decrease of ϵ_g. Such a decrease will occur only if the reaction is very fast, the stoichiometric coefficient is very high, and the feed is essentially pure reactant.

The second limiting form occurs when frictional losses in the downcomer dominate the accessories losses plus the kinetic energy change, and when flow in the downcomer is turbulent, so that $f_{dc} \cong$ constant. For this situation

$$\bar{v}_{dc} \cong \left(\frac{2g\epsilon_g L}{f_{dc}L_{dc}/D_{dc}} \right)^{1/2}$$

which reduces to the proportionality given by Eq. 16a when D_{dc} and (L/L_{dc}) are constant. For this case, which occurs when the riser and downcomer are very long, the liquid circulation rate does not depend on L.

Reaction in Gas Phase

Although the GLR is at steady state and the composition of the gas at any position in the riser is independent of time, the most convenient way to analyze the reaction in the bubble is from a Lagrangian viewpoint. The feed to the reactor is assumed to be a mixture of A, B and an inert (I). For a first-order, irreversible reaction taking place in an isothermal gas bubble

$$N_A = N_{A0}e^{-kt} \tag{17}$$

where N_A is the number of moles of component A in the bubble, t is the time (s) required for a bubble to move from the sparger ($z = 0$) to a height z, and $N_{A0} = N_A(t = 0)$, that is, N_{A0} is the number of moles in the bubble when it is formed at the sparger. The fractional conversion of A (X_A) defined by $X_A = (N_{A0} - N_A)/N_{A0}$, is used in this article to represent the progress of the reaction.

If the density in the gas-phase continuity equation for the riser is written using the ideal gas law, Eq. 2 becomes

$$\frac{\langle \bar{P} \rangle M_g \bar{\epsilon} \langle \bar{v}_g \rangle}{RT} = G \tag{18}$$

The molecular weight of the gas mixture at any time t is

$$M_g(t) = \frac{N_A M_A + N_B M_B + N_I M_I}{N_A + N_B + N_I}$$

where N_i is the number of moles of species i at time t ($i = A$, B, I), and M_i is the molecular weight of species i. The molecular weight of A (M_A) is equal to M_B/n, and the number of moles of B and A are related by stoichiometry, that is, $N_B = N_{B0} + (N_{A0} - N_A)/n$. Using these relationships together with Eq. 17 leads to

$$M_g(t) = \frac{M_B[x_{B0} + (x_{A0}/n)] + x_{I0}M_I}{1 + (1 - e^{-kt})x_{A0}[(1/n) - 1]} \tag{19}$$

where x_{i0} is the inlet mole fraction of species i.

The gas velocity can be expressed as the rate of change of axial position of a bubble with respect to time using Eq. 18

$$\langle \bar{v}_g \rangle = \frac{GRT}{\langle \bar{P} \rangle M_g \bar{\epsilon}} = \frac{dz}{dt}$$

Rearranging

$$\frac{dt}{dz} = \frac{\langle \bar{P} \rangle M_g \bar{\epsilon}}{GRT} \tag{20}$$

This equation has the time that the bubble has spent in the riser $t(z)$ as the dependent variable and the riser coordinate z as the independent variable. Equation 20 is subject to the initial condition $t = 0$ at $z = 0$. The overall residence time of the bubble in the riser t_f is the time that it takes for a bubble to rise from the sparger ($z = 0$) to the top of the riser ($z = L$).

Model Implementation

The procedure for solving the model equations is similar to that described by Sáez et al. (1998) with one basic modification. The Sáez et al. model requires the numerical solution of one ordinary differential equation, the liquid-phase momentum equation. In the new model with reaction in the gas phase, two ordinary differential equations must be solved: the liquid-phase momentum equation (Eq. 6) and the gas-phase continuity equation (Eq. 20). These two equations were integrated using the Runge-Kutta method with the boundary condition given by Eq. 10, and the initial condition $t = 0$ at $z = 0$.

The value of M_g was calculated from Eq. 19, and the values of $\bar{\epsilon}$, $\langle \bar{v}_g \rangle$, and $\langle \bar{v}_l \rangle$ were calculated as described in Sáez et al. (1998) at each step in the integration of Eqs. 6 and 20. The liquid mass flux in the riser L_f is not known *a priori* and an iterative procedure is required (Sáez et al., 1988). To start the solution, values of L_f and $\langle \bar{P} \rangle_{z=0}$ are assumed. The integration is then carried out. If the boundary condition at $z = L$ is not satisfied, $\langle \bar{P} \rangle_{z=0}$ is adjusted and the integration is repeated. Once this boundary condition is satisfied, the assumed and calculated values of L_f are compared and L_f is

adjusted if necessary. A solution is obtained when the assumed and calculated values of L_f are equal and, simultanously, the boundary condition at $z = L$ is satisfied.

One of the main advantages of the present model is its mathematical simplicity. A system of two ordinary differentials equations is solved in conjunction with four algebraic equations and the downcomer mechanical energy balance. The physical properties of the gas and liquid phases, the reactor dimensions, the gas superficial velocity, the bubble radius at the sparger, and the reaction parameters k and n are required as inputs. The model predicts the axial profiles for gas holdup, gas and liquid velocity, pressure and reactant conversion in the riser, as well as the liquid circulation flux, for the case of bubbly flow.

Results and Discussion

An analysis of the different variables that affect the operation of a GLR when a chemical reaction takes place was carried out using the model described above. Initially, the reaction was assumed to take place in a reactor with the dimensions shown in Figure 1 in order to study the effect of the stoichiometric coefficient (n), the kinetic rate constant (k), the bubble radius at the sparger (r_{b0}), and the inlet gas composition. Then, different scale-up strategies were studied, placing emphasis on changes of the inlet gas superficial velocity and the reactor dimensions. Finally, the model was used to simulate the coupling between hydrodynamics and chemical reaction in the experimental results of Amend (1992) with a KOH/CO_2 system.

Operating Conditions

The performance of an external-loop GLR must satisfy two main requirements: the desired conversion must be achieved, and it must be possible to remove or supply the heat of reaction. To obtain the desired conversion, the residence time of the gas in the reactor must be sufficiently long. The heat-transfer capability is related directly to the rate of liquid circulation in the reactor. In an external-loop GLR, the most logical place for a heat exchanger is in the downcomer. The liquid stream coming from the top of the riser and through the gas/liquid separator would enter the downcomer, exchange heat, and return to the bottom of the riser. The present model does not include heat exchange, except implicitly via the assumption of isothermal behavior. The rate of liquid circulation can also influence the ability to suspend a solid such as a catalyst, and it is one of the parameters that determines the residence time of the gas in the riser.

Base case

To analyze the effect of operating conditions on reactor performance and hydrodynamics, a base case was established. The base case is defined by: reactor dimensions, as shown in Figure 1; feed gas superficial velocity, $U_g^0 = 4.7$ cm/s; bubble radius at the sparger, $r_{b0} = 1$ mm (monodisperse bubbles); and inlet gas composition, pure reactant A, $x_{A0} = 1$. Two rate constants were considered: $k = 1.0\ s^{-1}$ (moderate reaction) and $k = 2.0\ s^{-1}$ (fast reaction). The stoichiometric coefficient n was taken to be 50 to allow substantial molar consumption of the gas phase. The molecular weight of A and the molecular weight of the inert I, when included, were taken to be 29. In the absence of inert, the results are independent of M_A. When inert is present, the results depend on the ratio M_I/M_A.

Stoichiometric coefficient and kinetic rate constant

The parameters k and n provide a mechanism to create changes in the hydrodynamics as a result of axial changes in the gas superficial velocity. Figures 2 to 6 present the effect of the stoichiometric coefficient n on the reactant conversion, bubble radius, gas holdup, and gas- and liquid-phase velocity profiles in the riser. These figures represent the base case conditions with a moderate reaction rate ($k = 1.0\ s^{-1}$).

Figure 2 shows the fractional conversion of Reactant A as a function of dimensionless axial position. The fractional conversion is not a unique function of axial position, but depends on the stoichiometric coefficient. This behavior results from the fact that liquid circulation rate depends on n. This causes the gas velocity, the gas holdup, and, ultimately, the gas residence time and the fractional conversion of A, to be functions of n. The relationships between these variables and the stoichiometric coefficient are developed below in more detail.

The effect of the stoichiometric coefficient on conversion is not as small as suggested by comparisons of X_A at fixed values of z/L. A different perspective is obtained by comparing the values of z/L required to achieve a given conversion. For example, the exit conversion at $z/L = 1$ for $n = 2$ is about 92%. This same conversion is achieved at $z/L \cong 0.90$ (about 10% less reactor volume) when $n = 5$ and at $z/L \cong 0.76$ (ca. 24% less reactor volume) when $n = 50$.

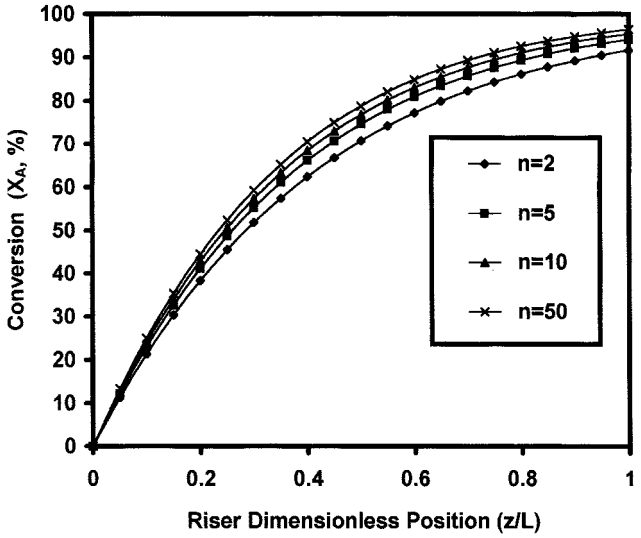

Figure 2. Effect of the stoichiometric coefficient *n* on the axial variation of the fractional conversion of Reactant *A*.

Base case, moderate reaction rate ($k = 1.0\ s^{-1}$).

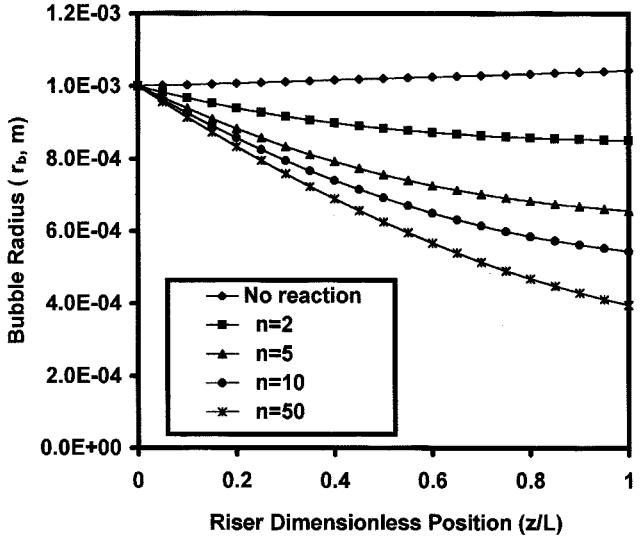

Figure 3. Effect of the stoichiometric coefficient *n* on the axial variation of the bubble radius.

Base case, moderate reaction rate ($k = 1.0\ s^{-1}$).

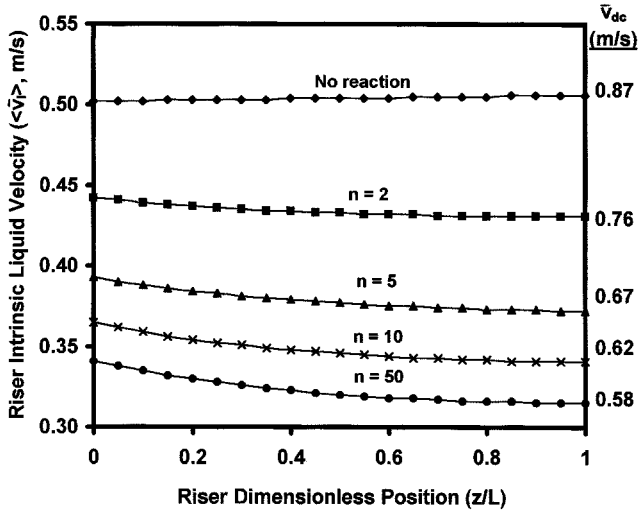

Figure 5. Effect of the stoichiometric coefficient *n* on the axial variation of the intrinsic riser liquid velocity.

Base case, moderate reaction rate ($k = 1.0\ s^{-1}$). $\bar{v}_{dc}$ is the average downcomer velocity.

Figure 3 shows axial profiles for the bubble radius in the riser. For the no-reaction case, the bubble radius increases slightly with z/L, as a result of the decrease in pressure along the riser. In the reactive cases ($n > 1$), the reduction in the gas volume as a result of the reaction dominates the effect of pressure, and the gas bubbles become smaller as z/L increases. The bubble radius reduction varies from about 10 to about 60% over the length of the column as n increases from 2 to 50 because the number of moles in the bubble decreases more per mole of A reacted as n increases.

Figure 4 presents the axial change in the gas holdup for different stoichiometric coefficients. Two aspects are worthy of special note. First, the gas holdup at the sparger ($z/L = 0$) for the reactive cases is always greater than for the no-reaction case. When reaction takes place, the liquid circulation rate decreases due to a lower global gas holdup, as shown in Eq. 16a. As the liquid velocity at the sparger decreases, the gas velocity at the sparger also decreases because the velocity of the gas relative to the liquid, ($\langle \bar{v}_g \rangle - \langle \bar{v}_l \rangle$), which depends only on the bubble radius and the physical properties of the phases, is constant. The gas continuity equation requires that the gas holdup increase when the gas velocity decreases. Second, the gas holdup at the sparger increases as n increases. This behavior results from the fact that the global gas holdup,

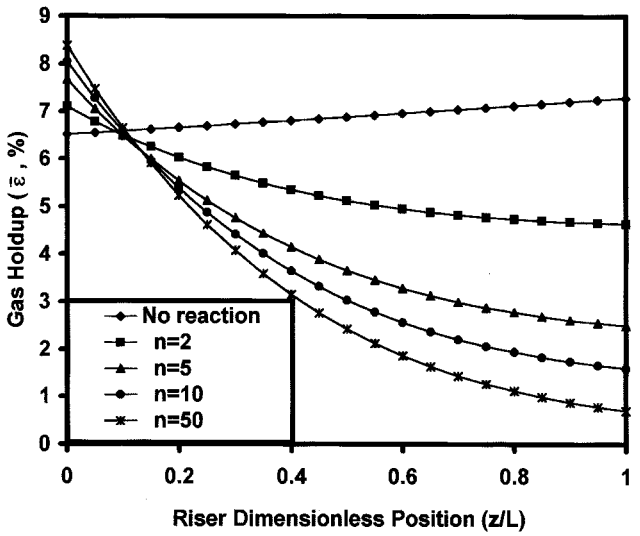

Figure 4. Effect of the stoichiometric coefficient *n* on the axial variation of the gas holdup.

Base case, moderate reaction rate ($k = 1.0\ s^{-1}$).

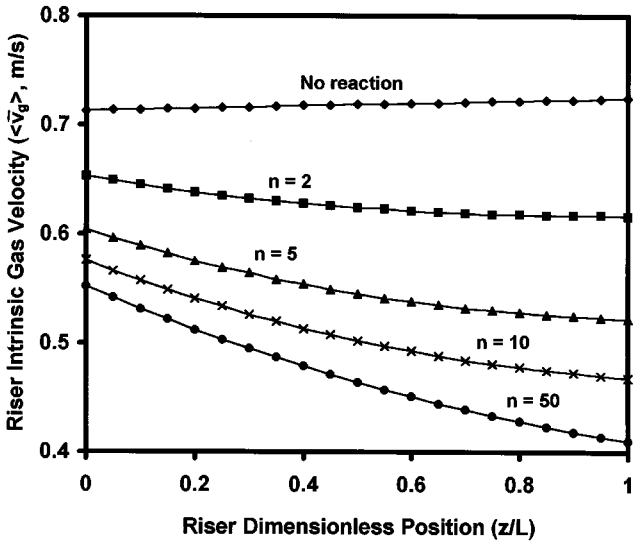

Figure 6. Effect of the stoichiometric coefficient *n* on the axial variation of the intrinsic riser gas velocity.

Base case, moderate reaction rate ($k = 1.0\ s^{-1}$).

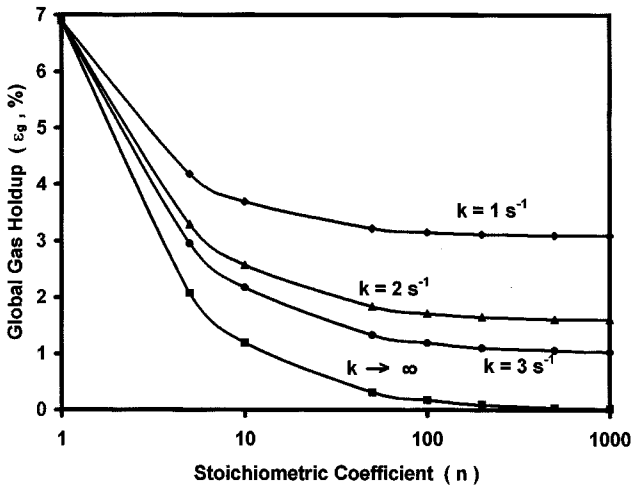

Figure 7. Effect of the rate constant *k* and the stoichiometric coefficient *n* on the global gas holdup.

Base case, semi-log scale.

and, consequently, the liquid flux, decrease as n increases. This causes the gas holdup at the sparger to increase with n, according to the previous argument.

Figure 5 shows that the liquid velocity in the riser is substantially lower for the reactive cases than for the no-reaction case, and that the intrinsic liquid velocity at any axial position decreases as n increases. The values of the average downcomer velocity $\bar{v}_{dc}$ are also shown in this figure. These values demonstrate the decrease in liquid circulation between the no-reaction and reactive cases, and with increasing n, as mentioned in the preceding paragraph.

Figure 6 shows that the intrinsic gas velocity in the riser is substantially lower for the reactive cases than for the no-reaction case, and that the gas velocity decreases with increasing n, at a fixed axial position. As gas velocity decreases, the residence time of the gas in the riser increases. This causes the conversion to increase with increasing n, as shown in Figure 2. The decrease in $\langle \bar{v}_g \rangle$ with increasing n is consistent with the fact that the holdup at the sparger increased with increasing n in Figure 4.

The previous examples showed the effect of n on the performance of a GLR, for a fixed value of k. Broader spectra of k and n values were studied, and some of the hydrodynamic results are presented in Figure 7, which shows the global gas holdup ϵ_g as a function of n for different k values. The value at $n = 1$ represents the no-reaction case. As k increases at constant n, the reaction is faster and ϵ_g is smaller. The curve for $k \to \infty$ is a limiting case where the reaction is instantaneous at the sparger. This case corresponds to a situation where there is no reaction, but the inlet superficial velocity is U_g^0/n. As n increases at constant k, ϵ_g decreases because each mole of A that reacts causes a larger decrease in the total moles in the bubble. For any value of k, there is no significant change in ϵ_g for n greater than about 100. When n is very large, the number of moles of gas that disappear is essentially equal to the number of moles of A that react. The existence of a finite global gas holdup as $n \to \infty$ reflects a kinetic limitation, that is, the bubbles require a finite residence time to reach complete conversion.

A consequence of the decrease of ϵ_g with increasing k and n is that the liquid circulation flux L_f (kg/m^2·s) is considerably lower for large values of k and n than for the no-reaction case. In fact, if the reaction is fast enough and if the reaction stoichiometry permits essentially complete gas consumption, the liquid circulation flux can approach zero.

Bubble radius at sparger

The function of the gas distributor is twofold: to create a uniform radial and angular profile of gas velocity, and to control the bubble-size distribution. The present model was used to study the effect of the bubble size at the sparger. Bubble radii ranging from 0.1 to 5 mm were considered. The range of bubble radii reported by several authors for different media in GLRs is between 1 and 3 mm (Fan, 1989; Chisti, 1989).

Figures 8 to 10 show the effect of the bubble radius at the sparger for the base case, moderate reaction ($k = 1.0$ s^{-1}; $n = 50$). The conversion of Reactant A is affected significantly by the initial bubble radius, as demonstrated in Figure 8. Since the relative bubble rise velocity, $(\langle \bar{v}_g \rangle - \langle \bar{v}_l \rangle)$ increases with bubble size, small bubbles rise more slowly and stay longer in the reactor, which causes the smallest bubbles to have the highest conversion at a fixed z/L. The exit conversion is about 83% when the bubble radius at the sparger is 5 mm. This same conversion is achieved at $z/L \cong 0.55$ when the bubble radius at the sparger is 1 mm, and at $z/L \cong 0.40$ when the bubble radius at the sparger is 0.1 mm.

Figure 9 shows the axial change of the gas holdup for different bubble radii. The gas holdup at $z/L = 0$ for small bubbles is much greater than for large bubbles, and the change in axial gas holdup for small bubbles is greater than that for large bubbles. The latter feature follows directly from Figure 8, which shows that the reactant conversion increases as the bubble size decreases at a fixed z/L. The gas holdup at the sparger is determined by the intrinsic gas velocity $\langle \bar{v}_g \rangle$ at the

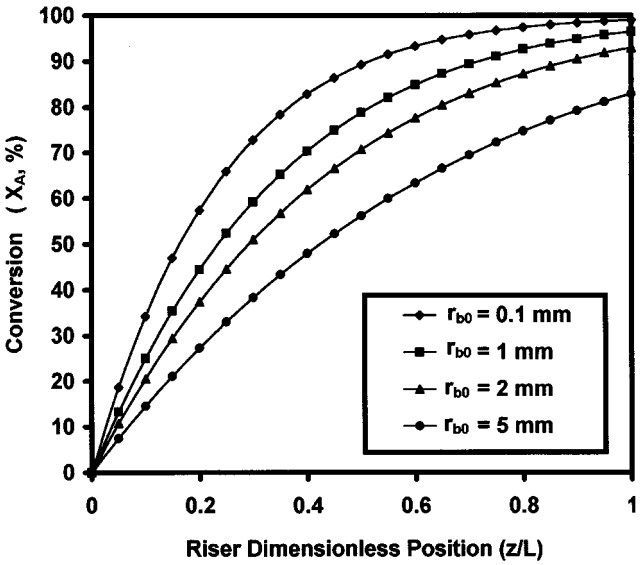

Figure 8. Effect of the bubble radius at the sparger on the axial variation of the fractional conversion of Reactant *A*.

Base case, moderate reaction rate ($k = 1.0$ s^{-1}, $n = 50$).

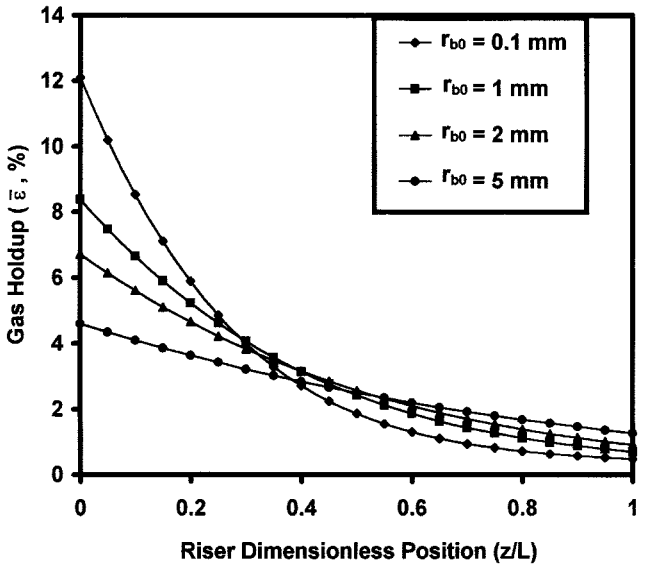

Figure 9. Effect of the bubble radius at the sparger on the axial variation of the gas holdup.

Base case, moderate reaction rate ($k = 1.0\ s^{-1}$, $n = 50$).

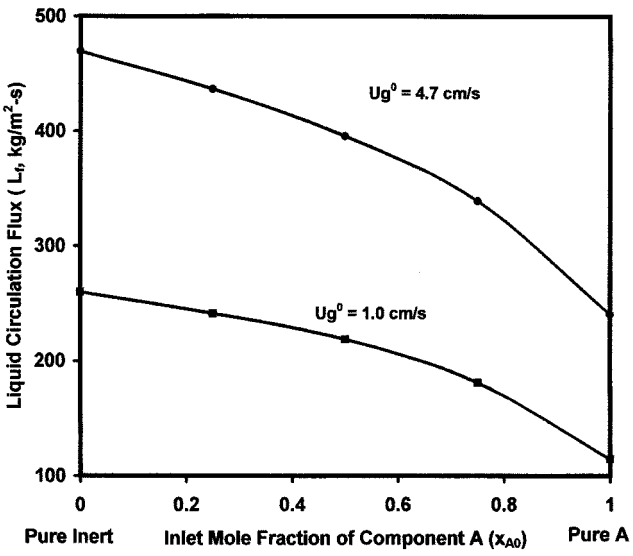

Figure 11. Effect of inlet gas composition on the liquid circulation flux.

Base case, fast reaction rate ($k = 2.0\ s^{-1}$, $n = 50$).

sparger. By continuity, the gas holdup will be low when $\langle \bar{v}_g \rangle$ is high for a fixed gas superficial velocity. As noted previously, the relative velocity ($\langle \bar{v}_g \rangle - \langle \bar{v}_l \rangle$) increases with bubble radius. A preliminary evaluation of the trend of $\langle \bar{v}_l \rangle$ with r_{b0} can be made by examining the gas holdup profiles in Figure 9. As a first approximation, it appears that ϵ_g is not highly sensitive to r_{b0}, since the higher values of $\bar{\epsilon}_{z=0}$ for the smaller bubbles are compensated by lower values of $\bar{\epsilon}$ in the top 60 to 70% of the riser. Thus, the higher holdups at $z/L = 0$ for the smaller bubbles appear to be caused primarily by their lower relative velocity.

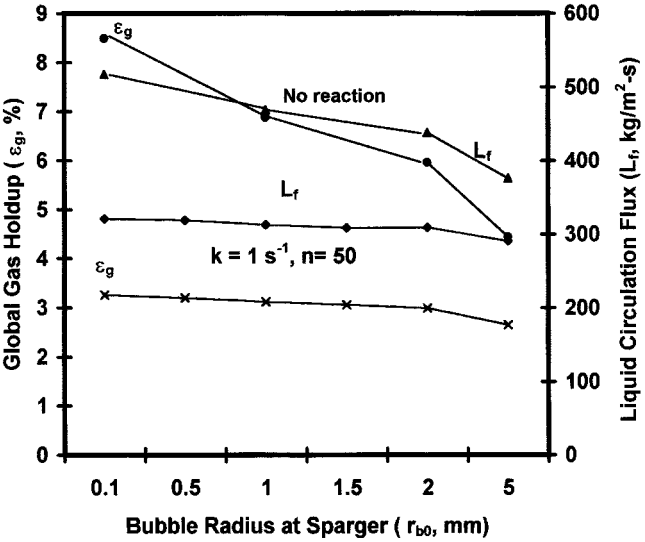

Figure 10. Effect of the bubble radius at the sparger on the liquid circulation flux and the global gas holdup.

Base case.

Figure 10 shows ϵ_g and L_f as a function of r_{b0}. Both ϵ_g and L_f are relatively weak functions of the bubble size when reaction takes place, validating the above analysis. The strongest dependence of ϵ_g and L_f on bubble size occurs when no reaction takes place. In this case, there is no molar gas consumption to compensate for the higher gas holdups at the sparger that are associated with the smaller bubbles.

Inlet gas composition

An inert component (or a reaction product) in the gas feed will ensure a minimum liquid circulation, even if the reactant is rapidly and completely consumed. Figure 11 shows the liquid flux as a function of the mole fraction of Reactant A in the feed for the base case, fast reaction ($k = 2.0\ s^{-1}$, $n = 50$) for two different superficial gas velocities. For both superficial velocities, L_f decreases by about 50% relative to the no-reaction case (pure inert) when pure A is fed. However, for a feed with 25% inert, the decrease with respect to the no-reaction case is only about 30%, and for a feed with 50% inert, the decrease is less than 20%.

Figure 12 shows the reactant conversion for different inlet gas compositions as a function of z/L for the base case, fast reaction. The fractional conversion at any axial position increases as the mole fraction of A in the feed increases. This result highlights a subtlety of the GLR operation. Since the liquid circulation rate decreases as x_{A0} increases, as shown in Figure 11, the time that it takes for a bubble to travel a specified distance increases as x_{A0} increases. This accounts for the increase in conversion at a fixed z/L with increasing x_{A0}.

Scale-up

Scaling of a reaction from the laboratory or pilot plant to industrial size is an important and sometimes complicated problem. Three different scale-up strategies were explored

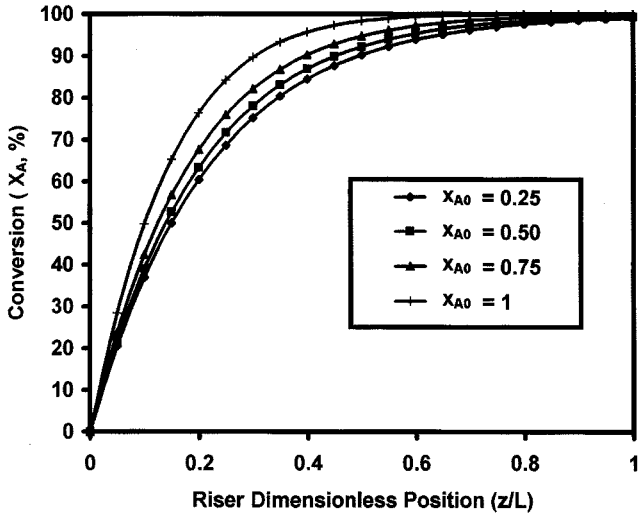

Figure 12. Effect of inlet gas composition on the fractional conversion of Reactant *A*.

Base case, fast reaction rate ($k = 2.0\ s^{-1}$, $n = 50$).

using the present model, primarily to provide a context for studying the effects of inlet gas superficial velocity and system dimensions.

In each case, the reactor volume and the inlet gas-flow rate were increased by the same factor, so that the apparent (superficial) gas residence time was constant. Strategy 1 consists of increasing the riser length, while keeping the diameter constant. Strategy 2 is to increase the reactor volume by increasing the riser diameter with the riser length held constant. This is normally a safe strategy, since the superficial gas velocity remains constant. However, from a practical point of view, it is not always possible or efficient to design reactors with very large diameters due to transportation limitations or the additional cost of on-site construction. This strategy also requires careful, sometimes elaborate, distributor designs. It is normally a costly strategy, especially for high-pressure reactors.

Strategies 1 and 2 represent extreme approaches to scale-up that establish limits of reactor behavior. An intermediate approach is to increase both L and D, keeping the L/D ratio constant. This strategy, Strategy 3, is a compromise that offers some of the advantages of the previous two.

There are two fundamental differences between the three scale-up strategies. First, the inlet gas superficial velocity increases in direct proportion to the reactor length. For a given scale-up, the superficial inlet gas velocity increases the most with Strategy 1, and does not increase at all with Strategy 2. Second, the hydraulic resistance in the downcomer circuit and the driving force for liquid circulation change in a different manner for the three strategies. These two differences will cause the reactor behavior to differ for the three strategies.

The three scale-up strategies were examined for three cases: (1) a pilot-scale reactor (Figure 1); (2) an intermediate, so-called ''semi-commercial'' scale; and (3) a large ''commercial'' scale. For the ''semi-commercial'' scale, the reactor volume and the gas feed rate were both a factor of 10 greater than for the pilot case. The scaling factor was 40 from the pilot case to the hypothetical ''commercial'' case. Table 1

Table 1. Scale-Up Analysis: Reactor Dimensions and Gas Superficial Velocities

	Scale						
	Base Case Pilot SF = 1	Hypothetical Semicommercial SF = 10*			Hypothetical Commercial SF = 40*		
Volume (m^3)	0.0445	0.445			1.78		
		Strategy No.‡			Strategy No.‡		
Variable		1	2	3	1	2	3
Riser length (m)**	1.56	15.6	1.56	3.36	62.4	1.56	5.34
Riser diameter (m)†	0.19	0.19	0.60	0.41	0.19	1.20	0.65
U_g^0 (m/s)$\times 10^2$	4.7	47	4.7	10	188	4.7	16

*SF = Scaling Factor = $\dfrac{\text{volume and volumetric gas feed rate of the scaled-up reactor}}{\text{volume and volumetric gas feed rate of the pilot reactor}}$.

**L_{do}/L = constant = 1.30.
†D/D_{dc} = constant = 1.36; $h_t = 2D$.
‡Strategy Number: 1—constant D; 2—constant L; 3—constant L/D.

contains a summary of the reactor dimensions and inlet gas superficial velocities for the three cases. All calculations were performed with $k = 0.50\ s^{-1}$ and $n = 50$.

Figure 13 shows dramatic differences in conversion for the three scales for Strategy 1. For the pilot GLR, the final conversion is about 74%. A major increase in conversion is observed as the scale increases; the final conversion is essentially 100% for both the semi-commercial and commercial reactors. The increase in conversion with increasing scale results from the fact that the actual residence time of a bubble in the riser t_f is not proportional to L/U_g^0. In fact, t_f increases substantially as L is increased. Increasing the superficial gas velocity at the sparger U_g^0 causes the gas holdup ϵ at the sparger to increase. Consequently, the gas velocity at the sparger $\langle \bar{v}_g \rangle_{z=0}$ does not increase in proportion to U_g^0.

Another way of understanding the results of Figure 13 is to recognize again that the gas velocity at the sparger $\langle \bar{v}_g \rangle_{z=0}$ is the sum of the liquid velocity at the sparger $\langle \bar{v}_l \rangle_{z=0}$ and the

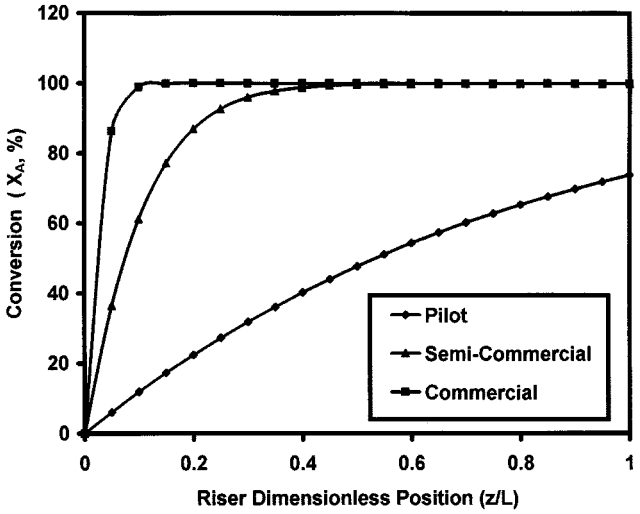

Figure 13. Scale-up analysis.

Axial conversion profile for Strategy 1 (constant L). $k = 0.5\ s^{-1}$, $n = 50$.

Table 2. Scale-Up Analysis: Global Gas Holdup and Liquid Circulation Flux

	Scale						
	Base Case Pilot SF = 1	Hypothetical Semicommercial SF = 10*			Hypothetical Commercial SF = 40*		
		Strategy No.**			Strategy No.**		
Variable†		1	2	3	1	2	3
ϵ_g (%)	4.7	4.0	4.2	5.0	3.5	3.8	4.7
L_f (kg/m^2·s)‡	382	523	429	575	506	435	708
L_fA (kg/s)	11	15	123	76	14	492	235
Conversion, X_A (%)	74	100	71	89	100	71	95

*SF = Scaling Factor = $\frac{\text{volume and volumetric gas feed rate of the scaled-up reactor}}{\text{volume and volumetric gas feed rate of the pilot reactor}}$.

**Strategy Number: 1—constant D; 2—constant L; 3—constant L/D.
†$k = 0.5\ s^{-1}$, $n = 50$.
‡Based on riser diameter.

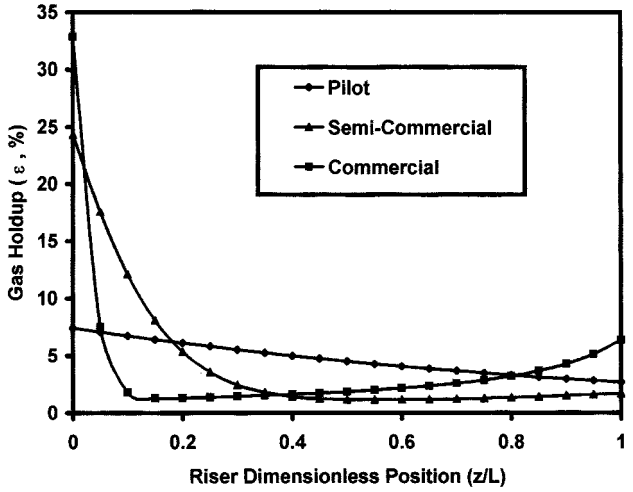

Figure 14. Scale-up analysis.

Axial gas holdup profile for Strategy 1 (constant D). $k = 0.5\ s^{-1}$, $n = 50$.

velocity of the gas relative to the liquid at the sparger ($\langle \bar{v}_g \rangle_{z=0} - \langle \bar{v}_l \rangle_{z=0}$). As noted previously, the latter is determined by the bubble radius at the sparger r_{b0} and the physical properties of the gas and liquid. However, $\langle \bar{v}_l \rangle_{z=0}$ depends on scale, since both ϵ and L_f depend on scale. For Strategy 1, L_f is about the same for the semi-commercial and commercial reactors, and is about 35% lower for the pilot scale. The semi-commercial and commercial reactors have essentially the same profile of the conversion of A as a function of *dimensional* length because the liquid velocity at the sparger is essentially the same for these two scales. The conversion for the pilot reactor is higher at a given value of z, because the liquid velocity at the sparger is lower. A detailed comparison of the results for Strategy 1 is shown in Table 2.

An interesting implication of Figure 13 is that the reactor volume may not have to be increased in proportion to the feed rate in order to achieve the desired conversion when Strategy 1 is used. If 74%, the outlet conversion for the pilot reactor, were the target conversion, the required values of z/L for the semi-commercial and commercial reactors would be about 0.14 and about 0.04, respectively. Thus, the required size of the semi-commercial reactor would be only about a factor of 1.4 greater than that of the pilot reactor, for a factor of 10 increase in production rate, and the required size of the commercial reactor would be only about a factor of 1.6 greater, for a factor of 40 increase in production rate. However, these factors are approximate. If the lengths of the semi-commercial and commercial reactors were reduced, the liquid circulation rate would change, creating changes in t_f and X_A.

Figure 14 presents the axial change in the gas holdup for Strategy 1. One of the problems that can occur with this strategy is evident when the holdups at the sparger ($z/L = 0$) are examined. For the semi-commercial and commercial reactors, these holdups are much higher than the normal range of GLR operation, and beyond the region of validity of the bubbly-flow assumption. The holdups at the sparger for these two cases are higher because the superficial gas velocity increases by factors of 10 and 40 respectively, relative to the pilot reactor. The holdup profile for the pilot reactor declines monotonically with z/L. However, the holdups for the semi-commercial and commercial cases go through minima and then increase with z/L as a result of expansion due to the large pressure variation over the tall columns.

As expected, the axial profiles of the reactant conversion and the gas holdup for Strategy 2 (constant reactor length) were almost identical regardless of scale. Minor differences between the pilot scale and the larger scales resulted from frictional effects, which became less important as the riser diameter increased. In fact, the results in Table 2 show that the conversion declined slightly as scale was increased for Strategy 2 because the liquid circulation rate increased with scale, resulting in a slight decrease of t_f.

Figures 15 and 16 show the axial profiles of conversion and gas holdup for Strategy 3. The semi-commercial and commercial conversions shown in Figure 15 are substantially lower than those for Strategy 1. However, the conversions for Strat-

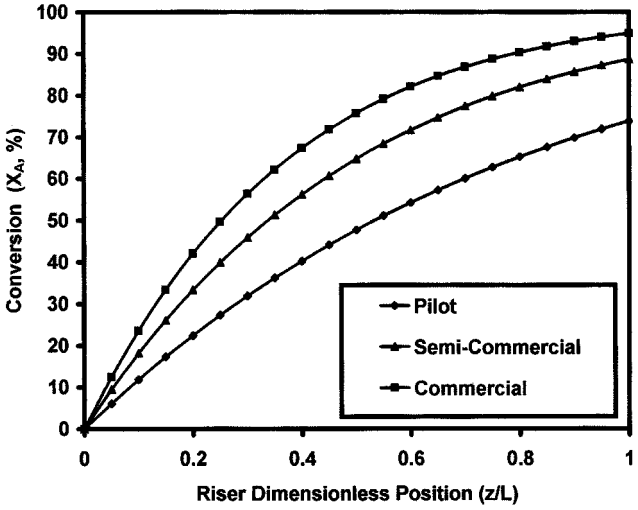

Figure 15. Scale-up analysis.

Axial gas holdup profile for Strategy 3 (constant L/D ratio). $k = 0.5\ s^{-1}$, $n = 50$.

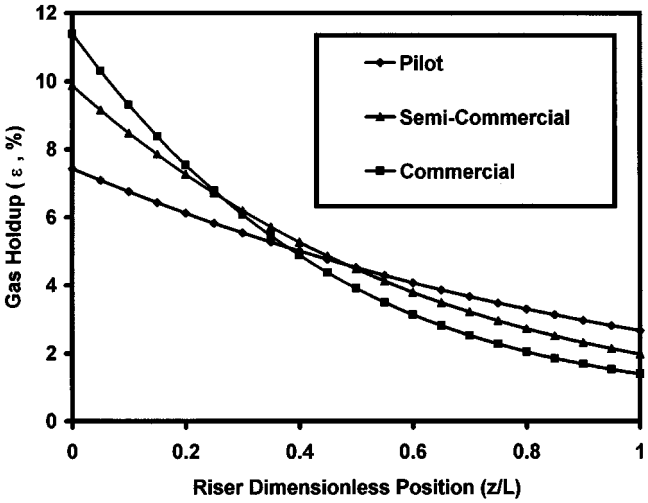

Figure 16. Scale-up analysis.

Axial gas holdup profile for Strategy 3 (constant L/D ratio). $k = 0.5\ s^{-1}$, $n = 50$.

egy 3 also increase with increasing scale, for the reasons discussed in connection with Strategy 1. The gas holdups in Figure 16 are within a normal range for GLRs (less than about 15%) and these profiles do not show a minimum with z/L.

Table 2 summarizes the global gas holdup, the conversion, the liquid circulation flux and total liquid flow ($L_f A$), for the three strategies. For Strategy 1, the liquid circulation flux L_f and the total liquid flow $L_f A$ increased less than 50% between the pilot and commercial scales. The failure of the total liquid flow to increase in direct proportion to scale might be a major concern in applications where a high rate of heat transfer was required.

For Strategy 1, L_f increases between the pilot and semi-commercial scales, despite the decrease in ϵ_g. This shows the influence of riser length L on liquid circulation, as suggested by Eq. 15. However, the increase in L_f between the pilot and semi-commercial scales is not nearly as large as predicted by Eq. 16b, since frictional losses in the downcomer are significant. The decrease in L_f between the semi-commercial and commercial reactors is close to that predicted by Eq. 16a.

The liquid circulation flux L_f is almost constant for Strategy 2, increasing slightly with scale as a result of reduced frictional losses in the downcomer. As a consequence, the total liquid flow $L_f A$ increases essentially in proportion to scale. The liquid circulation flux increases with scale for Strategy 3, but the increase in $L_f A$ is less than directly proportional to scale.

Comparison of Strategies 1, 2 and 3 appears to favor Strategy 1 from the standpoint of minimum reactor volume. However, the gas holdup for this strategy may fall well outside the region of validity for the present model and well outside the range of normal GLR operation for large reactors. Therefore, the theoretical volume advantages of this strategy may be difficult to achieve in practice. In addition, the failure of $L_f A$ to change significantly with scale could be a major disadvantage in applications requiring heat transfer. Strategy 2 is attractive because X_A does not depend significantly on scale, and because $L_f A$ scales directly with reactor volume. However, the construction of large-diameter reactors may be unattractive for the reasons previously mentioned. Strategy 3 may be a good compromise if Strategy 1 involves too much technical uncertainty, and Strategy 2 is too costly.

Finally, it should be emphasized that these scale-up calculations are intended to illustrate the phenomena that may arise when the inlet gas superficial velocity and/or the reactor dimensions are changed. The above results should not be generalized, or extrapolated to different situations, because of the specificity of these calculations, and the fact that the reaction considered is not a realistic representation of the reactions that are, or might be, run in a GLR.

Modeling the KOH/CO_2 System

The reactive absorption of CO_2 into concentrated, aqueous KOH solution is an example of a fast reaction with appreciable gas consumption along the riser. Even though the reaction occurs in the liquid phase and CO_2 is transferred from the gas to the liquid, the dominant source of coupling between the reaction and the reactor hydrodynamics is the decrease of gas superficial velocity along the riser. Therefore, the present model should be capable of describing the effect of CO_2 consumption on reactor hydrodynamics. However, the parameters k and n must be fitted to at least some of the experimental gas-holdup data so that the rate and extent of gas-phase mole change is properly matched.

The absorption of CO_2 into aqueous KOH was studied in the GLR shown in Figure 1 by Amend (1992). The cross-sectionally-averaged gas holdup was measured at four axial positions, and the downcomer liquid velocity was also measured.

The points in Figures 17a and 17b show that the measured gas holdup declined as CO_2 was consumed along the length of the reactor. For the two lowest gas superficial velocities, with the pure CO_2 feed (Figure 17a), the gas holdup was immeasurably low well below the top of the riser. Table 3 shows that the measured values of the average downcomer liquid velocity $\bar{v}_{dc}$ were substantially lower for the pure CO_2 feed than for the pure air feed. These data demonstrate many of the features predicted by the present model.

The parameters k and n were adjusted to fit the gas holdup profile along the riser for the case of 100% CO_2 feed. Figure 17a presents a comparison of the experimental and calculated gas holdup profiles for three different gas superficial velocities and a single set of k, n values: $k = 1.3\ s^{-1}$ and $n = 50$. The large value of n is a direct result of the large percentage decrease in holdup between the sparger and the top of the riser. A lower value of n would have overpredicted the gas holdups at $z/L = 1$.

The model with $k = 1.3\ s^{-1}$ and $n = 50$ was then tested against the data for the 50–50 vol. % air/CO_2 feed mixture, for which the gas holdup profiles were not as steep as for 100% CO_2. A comparison between the model and the experimental data is shown in Figure 17b. The fit is quite good, suggesting that a single pair of k, n values can describe gas holdup data over a range of superficial velocities gas compositions.

The downcomer liquid velocity, calculated with the model using the above values of k and n, is compared with the experimental data in Table 3. The model predicts the data rea-

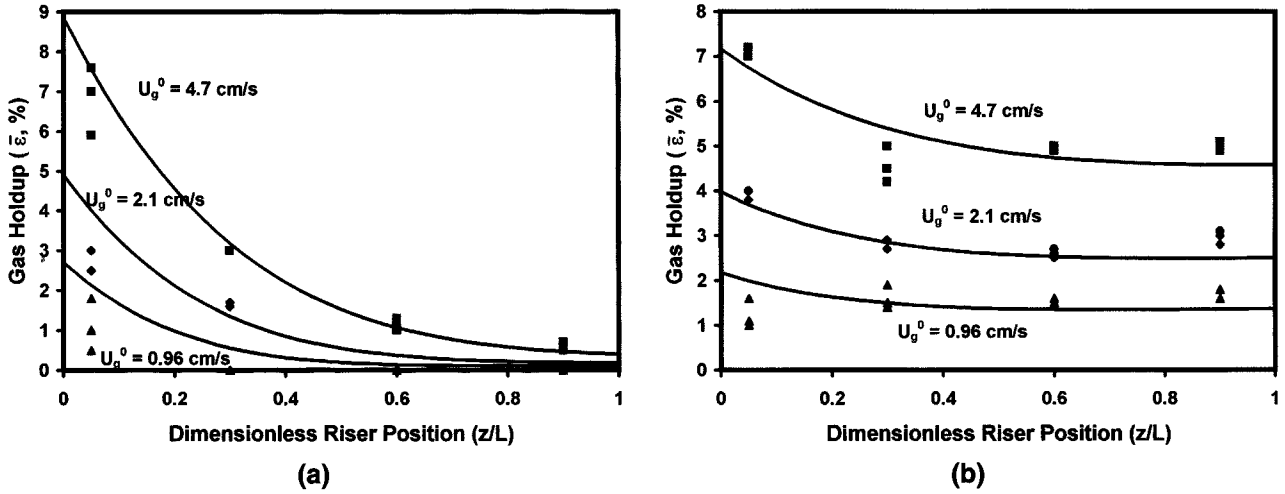

Figure 17. Comparison between the model and experimental holdup data for the KOH/CO_2 system for different inlet superficial velocities U_g^0.

(a) Inlet gas: pure CO_2; (b) inlet gas: 50–50 vol. % air-CO_2. ——: corresponds to the model with $k = 1.3\ s^{-1}$, $n = 50$; ■: experimental data for $U_g^0 = 4.7$ cm/s; ◆: experimental data for $U_g^0 = 2.1$ cm/s; ▲: experimental data for $U_g^0 = 0.96$ cm/s.

sonably well. As expected, the large molar gas consumption that occurred with pure CO_2 caused a significant decrease in the downcomer velocity.

Conclusions

A model that simulates the coupling of hydrodynamics and chemical reaction in a gas-lift reactor (GLR) has been developed based on a gas-phase, first-order, isothermal, irreversible reaction $nA \xrightarrow{k} B$ with no gas/liquid mass transfer. The axial profiles of reactant conversion, pressure, gas holdup, and gas and liquid velocity in the riser can be calculated, along with the liquid circulation rate. Consequently, the model is a useful tool for studying the variables that affect the design, scale-up and operation of GLRs. The liquid circulation flux is sensitive to the reaction rate and stoichiometry since these parameters have a major influence on the gas holdup profile in the riser, which drives liquid circulation. The use of feed gas mixtures that contain an inert (nonreacting) component can help to maintain liquid circulation, even when the reactant is completely consumed. The bubble size at the sparger has a substantial impact on the reactant conversion, but a relatively weak influence on the liquid circulation rate.

Different scale-up strategies were explored at a constant ratio of gas feed rate to reactor volume. The reactant conversion increased with scale, but the ratio of liquid circulation to gas feed rate decreased with scale, for scale-up strategies that involved increasing the superficial gas velocity, such as maintaining a constant diameter riser or maintaining a constant L/D ratio for the riser. The results for a strategy that involved maintaining a constant riser height and increasing the riser diameter were essentially insensitive to scale.

The model was able to describe gas holdup data for the KOH/CO_2 system at different gas superficial velocities and inlet gas compositions, using a single set of reaction parameters k and n. The measured liquid circulation rate was predicted adequately with this set of parameters.

Table 3. Downcomer Liquid Velocity ($\bar{v}_{dc}$) for KOH-CO_2 System

$U_g^0 \times 10^2$ (m/s)	Inlet Gas Composition	$\bar{v}_{dc}$ (m/s) Data	$\bar{v}_{dc}$ (m/s) Model
0.96	air	0.49	0.51
	50–50% air-CO_2	0.49	0.41
	100% CO_2	< 0.31**	0.25
2.1	air	0.64	0.65
	50–50% air-CO_2	0.61	0.55
	100% CO_2	< 0.31**	0.36
4.7	air	0.79	0.87
	50–50% air-CO_2	0.70	0.75
	100% CO_2	—	0.52

*Inlet superficial gas velocities.
**Minimum measurable value.

Notation

G = gas mass flux in riser, kg/m^2·s
k = kinetic rate constant for the reaction $nA \xrightarrow{k} B$, s^{-1}
L_{dc} = downcomer length, m
M_g = molecular weight of gas mixture, kg/kmol
ρ_i = phase density ($i = g, l$), kg/m^3
P_{atm} = atmospheric pressure, N/m^2
R = gas constant, m^3(N/m^2)/K·kmol
Re = Reynolds Number, based on bubble diameter and velocity of gas relative to liquid, $Re = 2r_b\rho_l(\langle\bar{v}_g\rangle - \langle\bar{v}_l\rangle)/\mu_l$
t_f = bubble residence time between sparger and top of riser, s
T = temperature, K
μ_l = liquid viscosity, kg/m·s
V = averaging volume, m^3
$\langle x\rangle$ = denotes volume average of x, defined by Eq. 3
$\langle\bar{x}\rangle$ = denotes cross-sectional average of $\langle x\rangle$ in the riser, defined by Eq. 4
x_i = mole fraction of component i in gas phase (i = A, B, I)

Literature Cited

Amend, R. J., ''Effect of Chemical Reactions on the Hydrodynamics of an Airlift Reactor,'' MS Thesis, Dept. of Chemical Engineering, North Carolina State University, Raleigh, NC (1992).

Chisti, Y., *Airlift Bioreactors*, Elsevier Applied Science, London (1989).

Chisti, Y., B. Halard, and M. Moo-Young, ''Liquid Circulation in Airlift Reactors,'' *Chem. Eng. Sci.*, **43**, 451 (1988).

Fan, L. S., *Gas-Liquid-Solid Fluidization Engineering*, Butterworths, Boston (1989).

Fleischer, C., S. Becker, and G. Eigenberger, ''Detailed Modeling of the Chemisorption of CO_2 into NaOH in a Bubble Column,'' *Chem. Eng. Sci.*, **51**, 1715 (1996).

Ghirardini, M., G. Donati, and F. Rivetti, ''Gas Lift Reactors: Hydrodynamics, Mass Transfer and Scale Up,'' *Chem. Eng. Sci.*, **47**, 2209 (1992).

Ishii, M., and N. Zuber, ''Drag Coefficient and Relative Velocity in Bubbly, Droplet or Particulate Flows,'' *AIChE J.*, **25**, 843 (1979).

Márquez, M. A., ''Modeling of Gas-lift Reactors: Coupling of Hydrodynamics, Mass Transfer and Chemical Reaction,'' PhD Thesis, Dept. of Chemical Engineering, North Carolina State University, Raleigh, NC (1999).

Merchuk, J. C., and Y. Stein, ''Local Hold-Up and Liquid Velocity in Air-Lift Reactors,'' *AIChE J.*, **27**, 377 (1981).

Sáez, A. E., M. A. Márquez, G. W. Roberts, and R. G. Carbonell, ''Hydrodynamic Model for Gas-Lift Reactors,'' *AIChE J.*, **44**, 1413 (1998).

Young, M. A., R. G. Carbonell, and D. F. Ollis, ''Airlift Bioreactors: Analysis of Local Two-Phase Hydrodynamics,'' *AIChE J.*, **37**, 403 (1991).

Manuscript received May 26, 1998, and revision received Dec. 7, 1998.